European Journal of Medicinal Chemistry 62 (2013) 1–10

Contents lists available at SciVerse ScienceDirect

European Journal of Medicinal Chemistry

journal homepage: http://www.elsevier.com/locate/ejmech

Original article

Design, synthesis and SAR of piperidyl-oxadiazoles as 11β-hydroxysteroid dehydrogenase 1 inhibitors

Guangxin Xia [a,b], Xiaodi You [a,b], Lin Liu [a,b], Haiyan Liu [b], Jianfa Wang [b], Yufang Shi [b], Ping Li [b], Bing Xiong [a,*], Xuejun Liu [b], Jingkang Shen [a,b,*]

[a] State Key Laboratory of Drug Research, Shanghai Institute of Materia Medica, Chinese Academy of Sciences, 555 Zuchongzhi Road, Zhangjiang Hi-Tech Park, Shanghai 201203, China
[b] Central Research Institute, Shanghai Pharmaceutical Holding Co., Ltd., 898 Halei Road, Zhangjiang Hi-Tech Park, Shanghai 201203, China

ARTICLE INFO

Article history:
Received 23 October 2012
Received in revised form
17 December 2012
Accepted 23 December 2012
Available online 10 January 2013

Keywords:
11β-HSD1 inhibitor
Oxadiazole
Bioisostere
SAR
Docking

ABSTRACT

The potential roles of 11β-HSD1 inhibitors in metabolic syndrome, T2D and obesity were well established and currently several classes of 11β-HSD1 inhibitors have been developed as promising agents against metabolic diseases. To find potent compounds with good pharmacokinetics, we used the bioisosterism approach, and designed the compound **2** and **3** bearing an 1,2,4-oxadiazole ring to replace the amide group in compound **1**. Guided by docking study, we then transformed compound **3** into a potent lead compound **4a** by changing sulfonamide group to amide. To elaborate this series of piperidyl–oxadiazole derivatives as human 11β-HSD1 inhibitors, we explored the structure–activity relationship of several parts of the lead compound. Based on their potency toward human 11β-HSD1 two compounds **4h** and **4q** were advanced to pharmacokinetic study. It was found that **4h** and **4q** are potent and selective human 11β-HSD1 inhibitors with better pharmacokinetic properties than those of the original piperidine-3-carboxamide compound **1**, and suitable for further *in vivo* preclinical study in primate model.

1. Introduction

Metabolic syndrome is defined as a collection of metabolic abnormalities including central obesity, insulin resistance, atherogenic dyslipidemia, hyperglycemia, and hypertension [1,2]. The prevalence of metabolic syndrome among the US adult population is more than 20%, and about 80% of type 2 diabetics (T2D) meet the criteria for the diagnosis of this disorder [1]. As a key risk factor for cardiovascular disease and T2D, metabolic syndrome has attracted numerous investigations on genes, proteins, pathways associated with this disease. Among them, glucocorticoid receptor (GR) signaling plays significant role in metabolic regulation [3–5]. GR signaling depends not only on the circulating cortisol levels but also on the intracellular production of cortisol through reduction of cortisone, the inactive glucocorticoid. The enzymes catalyzing the conversion between cortisone and cortisol are 11β-hydroxysteroid dehydrogenases (11β-HSDs). While the type 1 isoform (11β-HSD1), highly expressed in liver and adipose tissue, predominantly reduces cortisone to cortisol, the type 2 isoform (11β-HSD2), primarily expressed in kidney, oxidizes cortisol to cortisone [6]. The potential roles of 11β-HSD1 inhibitors in metabolic syndrome, T2D and obesity were established using transgenic mice, and accumulation of these findings has made 11β-HSD1 a promising target for metabolic disease [7–9].

In the past decade, several classes of 11β-HSD1 inhibitors have been published, including sulfonamides (e.g., BVT-14225), amides (e.g., PF-877423), triazoles (e.g., Merck 544), and thiazolones (e.g., AMG-221) [10–13]. In a phase II clinical trial, 11β-HSD1 inhibitor INCB-13739 (structure undisclosed) significantly improved insulin sensitivity in T2D patient who failed on metformin treatment and lowered triglyceride and cholesterol levels of patients with hyperlipidemia and hypertriglyceridemia [14]. Currently, other drugs such as PF-915275, MK-0916, and AZD-4071 are being evaluated in phase I/II trials for potential oral treatment of metabolic diseases [15–17].

Recently, we disclosed a series of sulfonamides represented by **1** (shown in Fig. 1), which showed high inhibitory activity against 11β-HSD1 but with poor liver microsome stability (HLM Clint 209 μL/min/mg protein) and low oral bioavailability in rats (F = 8%) [18]. As part of our continuing efforts on optimizing pharmacokinetics properties of this series, we incorporated the

* Corresponding authors. State Key Laboratory of Drug Research, Shanghai Institute of Materia Medica, Chinese Academy of Sciences, 555 Zuchongzhi Road, Zhangjiang Hi-Tech Park, Shanghai 201203, China. Tel.: +86 21 50806600x5407; fax: +86 21 50807088.
E-mail addresses: bxiong@mail.shcnc.ac.cn (B. Xiong), jkshen@mail.shcnc.ac.cn (J. Shen).

0223-5234/$ – see front matter © 2013 Elsevier Masson SAS. All rights reserved.
http://dx.doi.org/10.1016/j.ejmech.2012.12.059

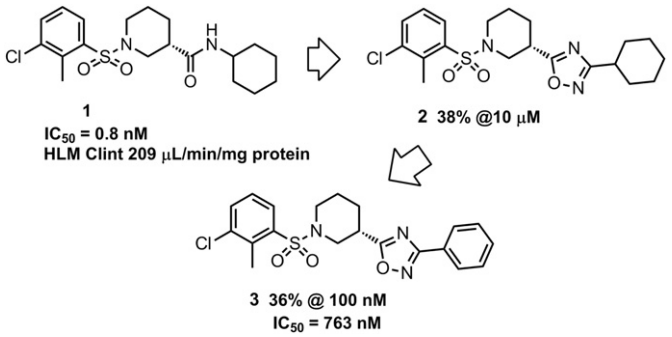

Fig. 1. Design and identification of piperidyl-oxadiazole 11β-HSD1 inhibitors.

readily constructed 1,2,4-oxadiazole ring, a known amide bioisostere [19], into the molecule to form compound **2**. Although **2** displayed very weak activity against human 11β-HSD1, interestingly, a simple replacement of cyclohexyl group of **2** with phenyl group led to compound **3** with moderate inhibition against human 11β-HSD1 (IC_{50} = 763 nM).

Utilizing **3** as a starting point, we designed and elaborated a series of piperidyl–oxadiazoles as 11β-HSD1 inhibitors with the approaches of docking and bioisosterism. In the present work, we report the lead identification and Structure–Activity Relationship (SAR) studies of this series.

2. Results and discussion

2.1. Docking study and lead identification

To investigate the binding mode of compound **3** with 11β-HSD1, the docking program Vina [20] was applied by using the crystal structure 3G49 as the template [21]. As obtained from docking study (shown in Fig. 2), compound **3** bound to 11β-HSD1 with the extended conformation. The 3-chloro-2-methyl benzene group is located in a subpocket lined with the residues Val-96, Leu-101 and Tyr-158. The oxygen atom of sulfonamide group is about 4.1 Å away from the oxygen atom of the side chain of Tyr-158. This docking study suggested that substitution of the sulfonamide group with its bioisostere amide group may render the ligand into linear shape, and may introduce a hydrogen bond between the ligand and Tyr-158. Therefore, we constructed a model compound and docked it into the binding site of 11β-HSD1. The result showed that it formed a hydrogen bond about 3.0 Å with the side chain of Tyr-158. To verify this, we synthesized the compound **4a**, a bioisostere of the compound **3**. Through the enzymatic inhibition assay, inhibitor **4a** (IC_{50} = 27 nM) is 28-fold more potent than compound **3**. Thus **4a** was selected as a promising hit of 11β-HSD1 for further exploring its structure–activity relationship.

2.2. Optimization and SAR study

Since we changed sulfonamide group to amide group, the ligand may interact to 11β-HSD1 enzyme with a different binding conformation. Therefore, we performed a systematic scan of **4a** type structure by varying its possible regio- and stereo-isomers. This yielded compounds **5**–**8** (Table 1). In consistent with previous studies, **4a** displayed the highest inhibition ratio of 77% at the ligand concentration of 100 nM, while other isomers showed considerably low inhibition ratios and were not considered for further SAR studies.

Next, we conducted a scaffold hopping on oxadiazole ring to prepare other five-member heterocycle linkers, including triazoles, tetrazole, and two other oxadiazoles. It is interested to found that,

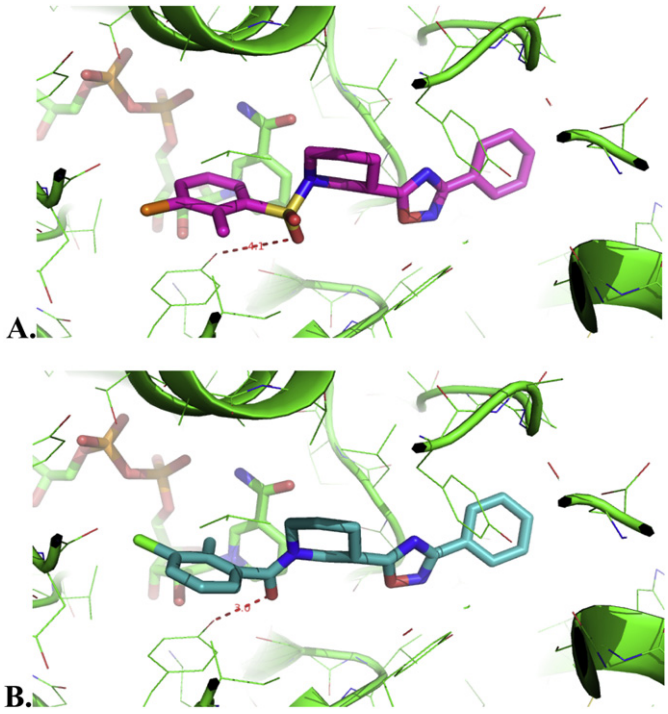

Fig. 2. The docking results of compound **3** (A) and **4a** (B). The crystal structure **3G49** was used as the template for docking study. The protein was shown in Ribbon scheme, and colored green. The NADPH, compound **3** and **4a** were shown in stick model, colored green, pink and cyan respectively. (For interpretation of the references to colour in this figure legend, the reader is referred to the web version of this article.)

although **13** has similar scaffold to **4a**, **4a** remains the best one in terms of potency toward human 11β-HSD1. As depicted in Table 2, introducing 4-methyl on triazole dramtically decreased the activity (**11** *vs.* **10**).

To explore the extensive SAR of **4a** series, more piperidyl-oxadiazole analogs have been prepared according to Schemes 1 and 2.

Syntheses of compounds with various R^1 groups were depicted in Scheme 1. (*S*)-Ethyl piperidine-3-carboxylate **15** was condensed with 3-chloro-2-methylbenzoic acid to produce ester **16**, which was hydrolysized to acid **17**. Various nitriles (**18a**–**h**) were reacted with hydroxylamine hydrochloride to afford N′-hydroxyimidamides **19a**–**h**. Target molecules (**14a**–**h**) were obtained via two consecutive steps: condensation of **19a**–**h** with **17** and intramolecular cyclization of intermediates **20a**–**h**.

Table 1
Human 11β-HSD1 activities of regionisomers and enantiomers on the piperidine core part.

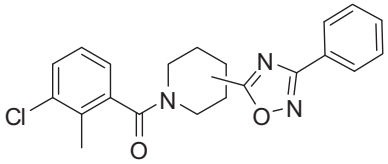

Compound	Substitution position and stero-configuration	Inhibition ratio[a]
4a	3S	77%
5	3R	2%
6	4	22%
7	2S	44%
8	2R	36%

[a] Note: The inhibition ratio is measured at ligand concentration 100 nM.

Table 2
Human 11β-HSD1 activities of the scaffold hopping toward oxadiazole core L.

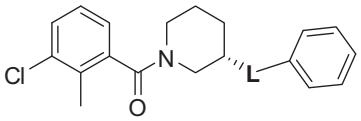

Compound	L	IC_{50} (nM)
9	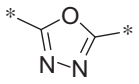	1316
10	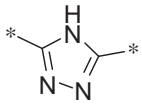	945
11	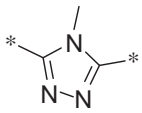	9%[a]
12	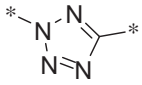	594
4a	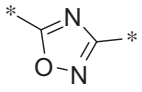	27
13	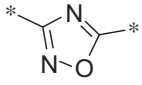	107

[a] Note: The inhibition ratio is measured at ligand concentration 100 nM.

Inhibitory activities of the target compounds against human 11β-HSD1 were determined [18]. As shown in Table 3, halogen substitution at various positions of benzene moiety decreased the activity against 11β-HSD1, especially at para-position (**14d** and **14h**). Changing the phenyl ring to cyclohexane ring or adamantly group also decreased the inhibitory activity (**14a** and **14b**). These all indicated that the benzene group at right hand moiety may fit well into the binding pocket.

Next, we modify the left hand moiety with various acyl groups, and the synthetic route is described in Scheme 2. N′-hydroxybenzimidamide **22**, obtained from benzonitrile **21** was reacted with hydroxylamine hydrochloride and condensed with Boc-(*S*)-piperidine-3-carboxylic acid to provide intermediate **23**. Intramolecular cyclization of **23** formed oxadiazole **24**, which was deprotected under acidic condition to afford the common intermediate **25**. Target compounds (**4a**–**w**) were produced by acylation of **25** with acyl chlorides or carboxylic acids.

The inhibitory activity toward human 11β-HSD1 of compounds **4a**–**x** is summarized in Table 4. Among the benzoic acid derivatives (**4a**–**i**), compound **4a** and **4g** had comparable activity. As indicated by docking study, the left hand moiety of **4a** is located in a hydrophobic sub-pocket, and the interaction between the benzene ring and 11β-HSD1 is matched very well. Interchange methyl and chloro-group was tolerated and showed no difference in potency (**4g** *vs.* **4a**). While substituting the chlorine of **4a** with iodine dramatically decreased the inhibitory activity (**4i**), compound **4h** with bromine substitution instead of chlorine displayed the best activity in this series with IC_{50} = 3.3 nM. However, regarding to the heteroaryl carboxylic acid derivatives (**4j**–**o**), all of them exhibited low activity with IC_{50} > 100 nM. In addition to this, the saturated ring derivatives were also investigated. There is no clear correlation between the ring size and the *in vitro* potency, and among them the cyclohexyl group compound **4q** was the best with the IC_{50} 71 nM.

Taking together of the SAR studies on analogs of **4a**, compound **4h** and **4q** were selected for further *in vitro* and *in vivo* evaluation. Compounds **4h** and **4q** displayed more than 1000 fold selectivity for human 11β-HSD1 over human 11β-HSD2 (**4h**: <50% inhibition at the concentration 10 μM *vs.* HSD2; **4q**: <50% inhibition at the concentration 100 μM *vs.* HSD2). Besides, both compounds were species-dependent inhibitors and showed less than 30% inhibitory activity against rodent 11β-HSD1 at a concentration of 1 μM.

2.3. DMPK study

To further assess the druglike properties of this series, we performed primary DMPK study on **4h** and **4q**, and the results were listed in Table 5. By comparing with the compound **1**, it was found that compounds **4h** and **4q** both showed good *in vitro* properties, including very weak inhibition to three P450 enzymes 3A4, 2D6 and 2C9 at the concentration 10 μM and better stability in human liver microsomes. The pharmacokinetic profile of **4h** and **4q** are also

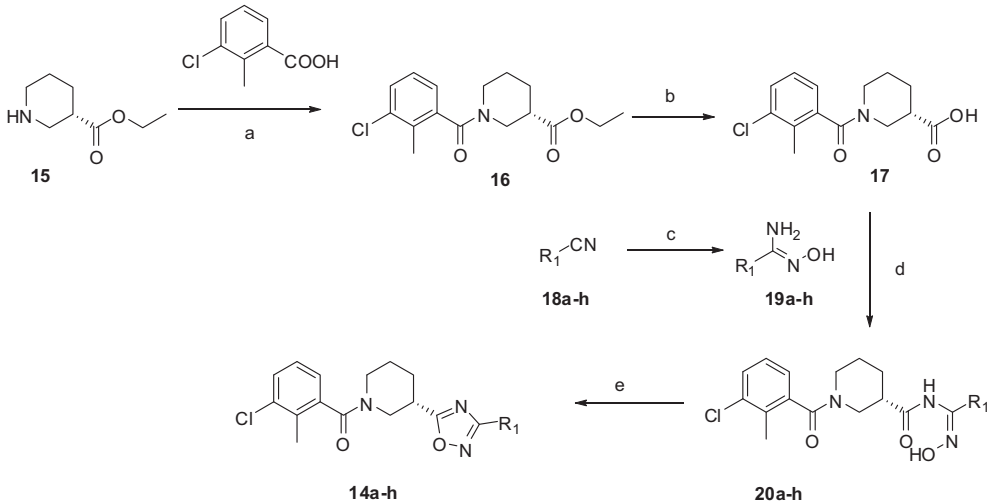

Scheme 1. Reagents and conditions: (a) EDCI·HCl, HOBT, DCM, rt, overnight, 86%; (b) 3 N aq. NaOH rt, 30 min, 99%; (c) NH_2OH·HCl, TEA, EtOH, 70 °C, 48 h, 74–100%; (d) EDCI·HCl, HOBT, dioxane, rt, overnight; (e) dioxane, 80 °C, overnight, 11–32% for two-steps.

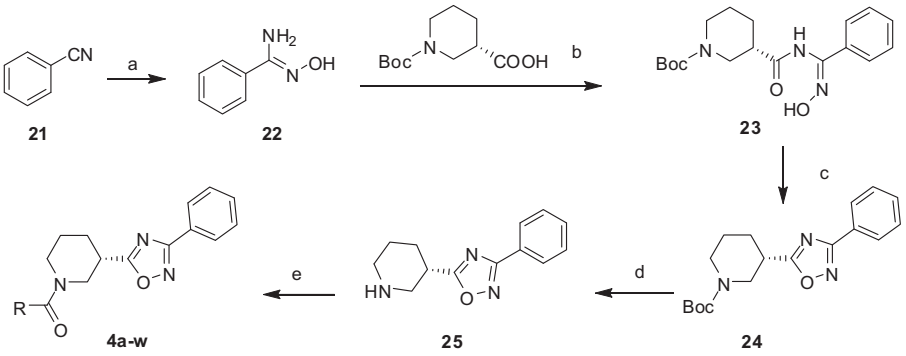

Scheme 2. Reagents and conditions: (a) $NH_2OH{\cdot}HCl$, TEA, EtOH, 75 °C, 12 h, 78%; (b) EDCI·HCl, HOBT, 1,4-dioxane, rt; (c) 1,4-dioxane, refluxed, overnight, 59% (two steps); (d) 4 N HCl-dioxane, DCM, rt, overnight, 86%; (e) RCOOH, EDCI·HCl, HOBT, DCM, rt, overnight, 51–87%.

Table 3
Human 11β-HSD1 activities of compounds with variable right hand moiety at R^1 group.

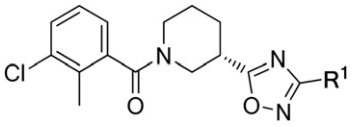

Compound	R^1	IC_{50} (nM)
4a	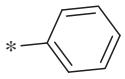	27
14a	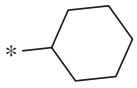	621
14b	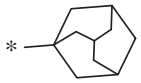	>1000
14c	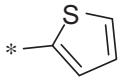	>1000
14d	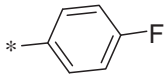	956
14e	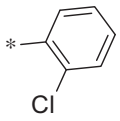	277
14f	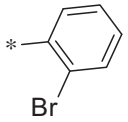	825
14g	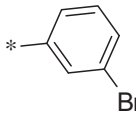	310
14h	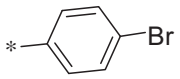	>1000

Table 4
Human 11β-HSD1 activities of compounds with different R^2 group at left hand moiety.

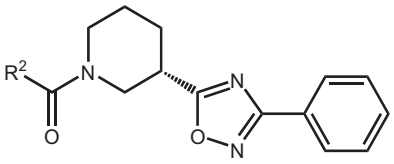

Compound	R^2	IC_{50} (nM) or inhibition ratio[a]
4a	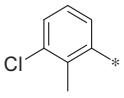	27
4b		2373
4c	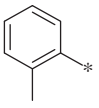	435
4d	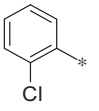	853
4e	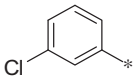	741
4f	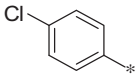	277
4g	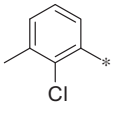	28
4h	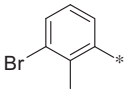	3.3
4i	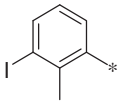	19%

Table 4 (*continued*)

Compound	R^2	IC_{50} (nM) or inhibition ratio[a]
4j		3%
4k	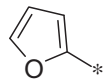	659
4l	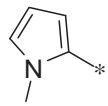	715
4m	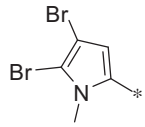	19%
4n	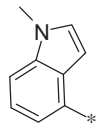	141
4o	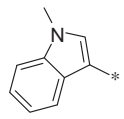	20%
4p	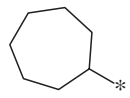	1484
4q	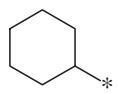	71
4r		326
4s		92
4t		793
4u	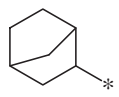	4%
4v	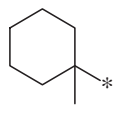	15%
4w	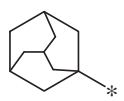	21%
4x	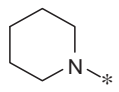	17%

[a] Note: The inhibition ratio is measured at ligand concentration 100 nM.

evaluated in rat. As shown in Table 5, **4h** and **4q** have higher bioavailability, longer half life, and slower clearance than compound **1**. The $T_{1/2}$ of **4h** is 2.1 h, about 5 times longer than compound **1**. Compound **4h** and **4q** are now being advanced to further PK/PD studies in primate models.

3. Conclusion

In conclusion, utilizing the concept of bioisosterism, we designed and elaborated a series of piperidyl-oxadiazole derivatives as human 11β-HSD1 inhibitors. On the basis of docking and primary SAR studies, compounds **4h** and **4q** were selected for pharmacokinetics study. It was found that **4h** and **4q** were potent and selective human 11β-HSD1 inhibitors with better pharmacokinetic properties than those of the original piperidine-3-carboxamide **1**, and suitable for further *in vivo* preclinical study in primate model.

4. Experimental

4.1. General

The reagents (chemicals) were purchased from Acros, Aldrich, Alfa-Aesar, TCI, Shanghai Chemical Reagent Company (SCRC) and Labpartner, and used without further purification. All non-aqueous reactions were performed in dried glassware under an atmosphere of Ar, unless otherwise specified. Yields were not optimized. Melting points were measured in capillary tube on a SGW X-4 melting point apparatus without correction. Nuclear magnetic resonance (NMR) spectra were performed on Varian Mercury-300 or 400 spectrometer. Chemical shifts were reported in parts per million (ppm, δ) downfield from tetramethylsilane. Proton coupling patterns were described as singlet (s), doublet (d), triplet (t), quartet (q), multiplet (m), doublet of doublets (dd), and broad (br). Elemental analyses were performed on an Elementar vario EL I analyzer. The LC-MS was carried out on Thermo Finnigan LCQDE-CAXP. Low-resolution mass spectra (LRMS) were produced by Finnigan MAT-95 and Finnigan LCQ Deca spectrometers and high resolution mass spectra (HRMS) were measured on Finnigan MAT 95 and MicroMass Q-Tof ultima mass spectrometers.

4.2. General procedure for the synthesis of target compounds ***14a–h***

4.2.1. (S)-Ethyl 1-(3-chloro-2-methylbenzoyl)piperidine-3-carboxylate (***16***)

To a stirred solution of 3-chloro-2-methylbenzoic acid (0.75 g, 4.4 mmol) in DCM (30 mL) was added (*S*)-ethyl piperidine-3-carboxylate (**15**, 0.63 g, 4.0 mmol), HOBT (0.54 g, 4.0 mmol) and EDCI·HCl (1.5 g, 8.0 mmol). The heterogeneous mixture was stirred at room temperature overnight, and washed successively with water (20 mL) and brine (20 mL × 2). The organic layer was dried over anhydrous Na_2SO_4, and concentrated to give the crude product, which was purified by flash chromatography (hexane/EtOAc = 1:1) afforded the ester intermediate as a colorless oil (1.07 g, 86%). ^{1}H NMR (300 MHz, $CDCl_3$): δ = 7.37 (d, J = 9.0 Hz, 1H), 7.17 (dd, J = 9.0, 8.9 Hz, 1H), 7.07 (d, J = 8.9 Hz, 1H), 4.18 (q, J = 7.1 Hz, 2H), 3.51–2.98 (m, 4H), 2.34–2.30 (m, 4H), 2.13–2.08 (m, 1H), 1.89–1.62 (m, 3H), 1.29 (t, J = 7.1 Hz, 3H); EI-MS : m/z 311 $[M + H]^+$.

4.2.2. (S)-1-(3-Chloro-2-methylbenzoyl)piperidine-3-carboxylic acid (***17***)

The obtained ester **16** (0.6 g) was dissolved in EtOH (15 mL), which was treated with aq. NaOH (3 N, 15 mL) and stirred at room temperature overnight. The solvent was evaporated at reduced pressure, the residue was dissolved in H_2O (25 mL), washed with

Table 5
In vitro and *in vivo* DMPK properties of selected compounds.

Compound	Microsomal stability clint (μL/min/mg protein)	%inhibition@10 μM			Rat PK[a]			
		3A4	2D6	2C9	iv CL L/min/kg)	po AUC_{0-t} (μM min)	po $T_{1/2}$ (h)	F (%)
4h	63	22	0	0	0.016	34.1	2.1	25
4q	44	7.7	12	16	0.024	25.3	1.3	36
1	209	73	34	16	0.130	11.3	0.4	8

[a] Note: iv dose of 3 mg/kg, po dose of 6 mg/kg, po vehicle: 1% CMC-Na in deionized water (suspension).

EtOAc (20 mL), acidified with aq. HCl (2 N), and extracted with DCM (50 mL × 3). The combined organic phase was dried over anhydrous Na_2SO_4 and evaporated to give product **17** as a white solid (0.54 g, yield 99%). ^{1}H NMR (300 MHz, $CDCl_3$): $\delta = 7.38$ (d, $J = 9.0$ Hz, 1H), 7.17 (dd, $J = 9.0$, 8.8 Hz, 1H), 7.05 (d, $J = 8.8$ Hz, 1H), 3.51–2.66 (m, 4H), 2.64–2.21 (m, 5H), 1.86–1.65 (m, 3H); EI-MS m/z: 282 $[M + H]^+$.

*4.2.3. Amide oxime **19a–h***

N′-Hydroxyimidamides (or amide oxime) **19a–h** was prepared from nitriles **18a–h** according to the same procedure described for compound **22** (see below). The crude products were confirmed by LC/MS (ESI) and used for the next step without further purification.

*4.2.4. General method of condensation and cyclization for **14a–h***

A solution of **17** (0.55 g, 2.0 mmol) in dry 1,4-dioxane (20 mL) at room temperature was charged with HOBt (0.27 g, 2.0 mmol), DIPEA (3.0 mmol) and EDCI·HCl (0.58 g, 3.0 mmol). After 30 min, an amide oxime **19a–h** (2.0 mmol) was added and the mixture was stirred until **17** had completely disappeared as monitored by LC-MS analysis. Then, the reaction mixture was refluxed overnight. After the solvent was removed, the solid residue was partitioned between EtOAc and water (1:1, 60 mL). The organic layer was separated, washed with water (15 mL) and 1 N NaOH (15 mL), dried with anhydrous Na_2SO_4 and concentrated under reduced pressure to give the crude product, which was purified by flash chromatography (hexane/EtOAc = 2:1) provided target oxadiazole (**14a–h**) in 11–32% yield.

*4.2.5. (S)-(3-Chloro-2-methylphenyl)(3-(3-cyclohexyl-1,2,4-oxadiazol-5-yl)piperidin-1-yl)methanone (**14a**)*

White solid (113 mg, yield 20%). ^{1}H NMR (300 MHz, $CDCl_3$): $\delta = 7.37$ (d, $J = 8.1$ Hz, 1H), 7.17 (dd, $J = 7.3$, 8.1 Hz, 1H), 7.09 (d, $J = 7.3$ Hz, 1H), 4.82, 4.66 and 4.37 (3× m, 1H), 3.67 and 3.45–3.15 (2× m, 3H), 3.03 (m, 1H), 2.75 (m, 1H), 2.36–2.26 (m, 4H), 2.03–1.91 (m, 3H), 1.85–1.64 (m, 5H), 1.57–1.25 (m, 5H); LC/MS (ESI): *m/z* 388.0 $[M + H]^+$; Anal. Calcd. for $C_{21}H_{26}ClN_3O_2$: C, 65.02; H, 6.76; N, 10.83; Found: C, 65.23; H, 6.85; N, 10.76.

*4.2.6. (S)-(3-Chloro-2-methylphenyl)(3-(3-(adamant-1-yl)-1,2,4-oxadiazol-5-yl)piperidin-1-yl)methanone (**14b**)*

White solid (140 mg, yield 32%). ^{1}H NMR (400 MHz, $CDCl_3$): $\delta = 7.38$ (d, $J = 7.7$ Hz, 1H), 7.18 (dd, $J = 7.3$, 7.7 Hz, 1H), 7.10 (d, $J = 7.3$ Hz, 1H), 4.82, 4.66 and 4.33 (3× m, 1H), 3.66 and 3.48–3.17 (2× m, 3H), 3.04 (m, 1H), 2.36–2.13 (m, 4H), 2.09–1.95 (m, 10H), 1.81–1.59 (m, 8H); LC/MS (ESI): *m/z* 439.9 $[M + H]^+$; HRMS-ESI: *m/z* $[M + H]^+$ calcd for $C_{25}H_{31}ClN3O_2^+$: 440.2099, found: 440.2105.

*4.2.7. (S)-(3-Chloro-2-methylphenyl)(3-(3-(thiophen-2-yl)-1,2,4-oxadiazol-5-yl)piperidin-1-yl)methanone (**14c**)*

White solid (95 mg, yield 12%). ^{1}H NMR (300 MHz, $CDCl_3$): $\delta = 7.75$ (m, 1H), 7.49 (m, 1H), 7.36 (m, 1H), 7.19–7.06 (m, 3H), 4.84, 4.63 and 4.26 (3× m, 1H), 3.71 and 3.45 (2× m, 2H), 3.29 and 3.07 (2× m, 2H), 2.38–2.24 (m, 4H), 2.05–1.45 (m, 3H); LC/MS (ESI): *m/z* 388.0 $[M + H]^+$; Anal. Calcd. for $C_{19}H_{18}ClN_3O_2S$: C, 58.83; H, 4.68; N, 10.83; Found: C, 58.66; H, 4.64; N, 10.59.

*4.2.8. (S)-(3-Chloro-2-methylphenyl)(3-(3-(4-fluorophenyl)-1,2,4-oxadiazol-5-yl)piperidin-1-yl)methanone (**14d**)*

White solid (110 mg, yield 14%). ^{1}H NMR (300 MHz, $CDCl_3$): $\delta = 8.11–7.97$ (m, 2H), 7.37 (m, 1H), 7.21–7.06 (m, 4H), 4.85, 4.62 and 4.35 (3× m, 1H), 3.74 and 3.46 (2× m, 2H), 3.29 and 3.07 (2× m, 2H), 2.38–2.26 (m, 4H), 2.04–1.48 (m, 3H); LC/MS (ESI): *m/z* 400.0 $[M + H]^+$; Anal. Calcd. for $C_{21}H_{19}ClFN_3O_2$: C, 63.08; H, 4.79; N, 10.51; Found: C, 63.27; H, 4.84; N, 10.65.

*4.2.9. (S)-(3-Chloro-2-methylphenyl)(3-(3-(2-chlorophenyl)-1,2,4-oxadiazol-5-yl)piperidin-1-yl)methanone (**14e**)*

White solid (102 mg, yield 12%). ^{1}H NMR (300 MHz, $CDCl_3$): $\delta = 7.91$ (m, 1H), 7.55 (m, 1H), 7.42–7.38 (m, 3H), 7.20–7.10 (m, 2H), 4.88, 4.67 and 4.36 (3× m, 1H), 3.77 and 3.46 (2× m, 2H), 3.35 and 3.12 (2× m, 2H), 2.38–2.28 (m, 4H), 2.01–1.54 (m, 3H); LC/MS (ESI): *m/z* 415.8 $[M + H]^+$; HRMS-ESI: *m/z* $[M + H]^+$ calcd for $C_{21}H_{20}Cl_2N_3O_2^+$: 416.0927, found: 416.0934.

*4.2.10. (S)-(3-(3-(2-Bromophenyl)-1,2,4-oxadiazol-5-yl)piperidin-1-yl)(3-chloro-2-methylphenyl)methanone (**14f**)*

White solid (100 mg, yield 11%). ^{1}H NMR (400 MHz, $CDCl_3$): $\delta = 7.87–7.71$ (m, 2H), 7.44–7.34 (m, 3H), 7.20–7.10 (m, 2H), 4.88, 4.67 and 4.33 (3× m, 1H), 3.79–3.03 (m, 4H), 2.38–2.27 (m, 4H), 2.04–1.59 (m, 3H); LC/MS (ESI): *m/z* 459.7 $[M + H]^+$; HRMS-ESI: *m/z* $[M + Na]^+$ calcd for $C_{21}H_{19}BrClN_3C_{21}H_{19}BrClN_3NaO_2^+$: 482.0241, found: 482.0221.

*4.2.11. (S)-(3-(3-(3-Bromophenyl)-1,2,4-oxadiazol-5-yl)piperidin-1-yl)(3-chloro-2-methylphenyl)methanone (**14g**)*

Primrose yellow solid (289 mg, yield 31%). ^{1}H NMR (400 MHz, $CDCl_3$): $\delta = 8.22$ (m, 1H), 7.99 (m, 1H), 7.64 (m, 1H), 7.40–7.32 (m, 2H), 7.20–7.08 (m, 2H), 4.86, 4.67 and 4.31 (3× m, 1H), 3.75 and 3.48 (2× m, 2H), 3.32 and 3.11 (2× m, 2H), 2.38–2.27 (m, 4H), 2.04–1.54 (m, 3H); LC/MS (ESI): *m/z* 459.7 $[M + H]^+$; HRMS-ESI: *m/z* $[M + H]^+$ calcd for $C_{21}H_{20}BrClN_3O_2^+$: 460.0422, found: 460.0420.

*4.2.12. (S)-(3-(3-(4-Bromophenyl)-1,2,4-oxadiazol-5-yl)piperidin-1-yl)(3-chloro-2-methylphenyl)methanone (**14h**)*

Primrose yellow solid (290 mg, yield 31%). ^{1}H NMR (400 MHz, CDCl3): $\delta = 7.96$ (m, 1H), 7.88 (m, 1H), 7.65–7.59 (m, 2H), 7.38 (m, 1H), 7.22–7.06 (m, 2H), 4.84, 4.68 and 4.33 (3× m, 1H), 3.72 and 3.47 (2× m, 2H), 3.31 and 3.10 (2× m, 2H), 2.38–2.27 (m, 4H), 2.02–1.63 (m, 3H); LC/MS (ESI): *m/z* 459.8 $[M + H]^+$; HRMS-ESI: *m/z* $[M + H]^+$ calcd for $C_{21}H_{20}BrClN_3O_2^+$: 460.0422, found: 460.0417.

*4.3. General procedure for the synthesis of target compounds **14a–w***

*4.3.1. N′-Hydroxybenzimidamide (**22**)*

Triethylamine (42 mL, 0.3 mol) was added to a solution of benzonitrile (**21**, 10.3 g, 0.1 mol), hydroxylamine hydrochloride (20.9 g, 0.3 mol) and ethanol (150 mL) and stirred for 12 h at 75 °C. The reaction mixture was cooled to room temperature and evaporated to dryness, extracted with DCM (300 mL)/water (100 mL). The organic layer dried with MgSO4, filtered and evaporated to dryness

yielding the desired product **22** as a primrose yellow liquid (10.6 g, yield 78%). ^{1}H NMR (300 MHz, DMSO-d_6): δ = 9.59 (s, 1H), 7.62–7.67 (m, 2H), 7.32–7.37 (m, 3H), 5.77 (s, 2H); LC/MS (ESI): *m/z* 137 $[M + H]^+$.

*4.3.2. (S)-tert-Butyl 3-(3-phenyl-1,2,4-oxadiazol-5-yl)piperidine-1-carboxylate (**24**)*

A solution of (*S*)-1-(tert-butoxycarbonyl)piperidine-3-carboxylic acid (5.05 g, 22 mmol) in dry 1,4-dioxane (50 mL) at room temperature was charged with HOBt (2.97 g, 22 mmol) and EDCI·HCl (6.34 g, 33 mmol). After 30 min, **22** (3.0 g, 22 mmol) was added and the mixture was stirred until starting material had completely disappeared as monitored by LC-MS analysis. Then, the reaction mixture was refluxed overnight. After the solvent was removed, the solid residue was partitioned between EtOAc and water (1:1, 150 mL). The organic layer was separated, washed with water (50 mL) and 1 N NaOH (50 mL), dried over anhydrous Na_2SO_4 and concentrated under reduced pressure to give the crude product, which was purified by flash chromatography (hexane/EtOAc = 2:1) provided **24** as a white solid (4.28 g, yield 59%). $[\alpha]_D^{20}$ = +76.6 (*c* = 1.0 in CH_2Cl_2); ^{1}H NMR (400 MHz, $CDCl_3$): δ = 8.08–8.06 (m, 2H), 7.49–7.46 (m, 3H), 4.28 (br s, 1H), 3.98 (m, 1H), 3.33 (br s, 1H), 3.15 (m, 1H), 2.98 (m, 1H), 2.25 (m, 1H), 1.92–1.81 (m, 2H), 1.60 (m, 1H), 1.46 (s, 9H); ^{13}C NMR (100 MHz, $CDCl_3$): δ = 179.93, 168.25, 154.52, 131.17, 128.84 (2C), 127.46 (2C), 126.81, 80.06, 46.73 (br s, 1C), 43.68 (br s, 1C), 34.87, 28.59, 28.41 (3C), 23.98 (br s, 1C); LC/MS (ESI): *m/z* 352 $[M + Na]^+$.

*4.3.3. (S)-3-Phenyl-5-(piperidin-3-yl)-1,2,4-oxadiazole (**25**)*

To a solution of **24** (3.7 g, 11 mmol) in DCM (30 mL) was added 4 N HCl in dioxane (10 mL). The resulting mixture was stirred at rt overnight. Water (50 mL) was added, and the mixture was washed with DCM (30 mL × 2). The aqueous phase was basified with 2 N aq. NaOH to pH = 9∼10, and extracted with EtOAc (100 mL × 2). The combined organic phase was dried over anhydrous $MgSO_4$, and concentrated under reduced pressure to afford the product as a primrose yellow oil (2.2 g, yield 86%), which was used for the next step without further purification. LC/MS (ESI): *m/z* 230 $[M + H]^+$.

*4.3.4. General method of condensation for target compounds **4a**–**w***

To a stirred solution of **25** (115 mg, 0.5 mmol) in DCM (10 mL) was added carboxylic acid (0.5 mmol), HOBT (68 mg, 0.5 mmol) and EDCI·HCl (144 mg, 0.75 mmol). The mixture was stirred at room temperature overnight, and washed successively with water (5 mL) and brine (10 mL × 2). The organic layer was dried over anhydrous Na_2SO_4, and concentrated to give the crude product, which was purified by flash chromatography (hexane/EtOAc = 3:1–1:1) afforded **4a**–**w**.

*4.3.5. (S)-(3-Chloro-2-methylphenyl)(3-(3-phenyl-1,2,4-oxadiazol-5-yl)piperidin-1-yl)methanone (**4a**)*

White solid (139 mg, 73%). $[\alpha]_D^{20}$ = +65.8 (*c* = 0.35 in CH_2Cl_2); ^{1}H NMR (300 MHz, $CDCl_3$): δ = 8.09 (m, 1H), 8.01 (m, 1H), 7.52–7.44 (m, 3H), 7.37 (m, 1H), 7.21–7.07 (m, 2H), 4.89–4.33 (m, 1H), 3.79–3.08 (m, 4H), 2.39–2.28 (m, 4H), 2.04–1.70 (m, 3H); LC/MS (ESI): *m/z* 381.9 $[M + H]^+$; HRMS-ESI: *m/z* $[M + Na]^+$ calcd for $C_{21}H_{20}ClN_3NaO_2^+$: 404.1136, found: 404.1161.

*4.3.6. (S)-Phenyl(3-(3-phenyl-1,2,4-oxadiazol-5-yl)piperidin-1-yl)methanone (**4b**)*

Colorless oil (93 mg, yield 56%). ^{1}H NMR (400 MHz, $CDCl_3$): δ = 8.07 (m, 2H), 7.49–7.47 (m, 3H), 7.42 (m, 5H), 4.91 and 4.44 (2× m, 1H), 4.08 and 3.78 (2× m, 1H), 3.50–3.17 (m, 3H), 2.35 (m, 1H), 2.04–1.68 (m, 3H); LC/MS (ESI): *m/z* 333.9 $[M + H]^+$; HRMS-ESI: *m/z* $[M + Na]^+$ calcd for $C_{20}H_{19}N_3NaO_2^+$: 356.1369, found: 356.1367.

*4.3.7. (S)-(3-(3-Phenyl-1,2,4-oxadiazol-5-yl)piperidin-1-yl)(o-tolyl)methanone (**4c**)*

Colorless oil (112 mg, yield 65%). ^{1}H NMR (400 MHz, $CDCl_3$): δ = 8.10 (m, 1H), 8.00 (m, 1H), 7.50–7.43 (m, 3H), 7.29–7.20 (m, 4H), 4.93, 4.66 and 4.45 (3× m, 1H), 3.79 and 3.46 (2× m, 2H), 3.30 and 3.10 (2× m, 2H), 2.37–2.26 (m, 4H), 2.04–1.58 (m, 3H); LC/MS (ESI): *m/z* 347.9 $[M + H]^+$; HRMS-ESI: *m/z* $[M + Na]^+$ calcd for $C_{21}H_{21}N_3NaO_2^+$: 370.1526, found: 370.1524.

*4.3.8. (S)-(2-Chlorophenyl)(3-(3-phenyl-1,2,4-oxadiazol-5-yl)piperidin-1-yl)methanone (**4d**)*

White solid (148 mg, yield 81%). ^{1}H NMR (400 MHz, $CDCl_3$): δ = 8.11 (m, 1H), 8.03 (m, 1H), 7.55–7.44 (m, 3H), 7.41 (m, 1H), 7.34–7.26 (m, 3H), 5.06, 4.97, 4.83 and 4.39 (4× m, 1H), 3.80–2.95 (m, 4H), 2.36 (m, 1H), 2.04–1.68 (m, 3H); LC/MS (ESI): *m/z* 367.9 $[M + H]^+$; HRMS-ESI: *m/z* $[M + Na]^+$ calcd for $C_{20}H_{18}ClN_3NaO_2^+$: 390.0980, found: 390.0973.

*4.3.9. (S)-(3-Chlorophenyl)(3-(3-phenyl-1,2,4-oxadiazol-5-yl)piperidin-1-yl)methanone (**4e**)*

Colorless oil (115 mg, yield 63%). ^{1}H NMR (400 MHz, $CDCl_3$): δ = 8.06 (m, 2H), 7.50–7.46 (m, 3H), 7.43–7.30 (m, 4H), 4.82–3.96 (m, 2H), 3.68–3.13 (m, 3H), 2.34 (m, 1H), 2.03–1.62 (m, 3H); LC/MS (ESI): *m/z* 367.9 $[M + H]^+$; HRMS-ESI: *m/z* $[M + Na]^+$ calcd for $C_{20}H_{18}ClN_3NaO_2^+$: 390.0980, found: 390.0979.

*4.3.10. (S)-(4-Chlorophenyl)(3-(3-phenyl-1,2,4-oxadiazol-5-yl)piperidin-1-yl)methanone (**4f**)*

White solid (135 mg, yield 74%). ^{1}H NMR (300 MHz, $CDCl_3$): δ = 8.05 (m, 2H), 7.50–7.44 (m, 3H), 7.42–7.34 (m, 4H), 7.43–7.32 (m, 4H), 4.82–3.73 (m, 2H), 3.57–3.16 (m, 3H), 2.33 (m, 1H), 2.03–1.64 (m, 3H); LC/MS (ESI): *m/z* 367.9 $[M + H]^+$; HRMS-ESI: *m/z* $[M + Na]^+$ calcd for $C_{20}H_{18}ClN_3NaO_2^+$: 390.0980, found: 390.0965.

*4.3.11. (S)-(2-Chloro-3-methylphenyl)(3-(3-phenyl-1,2,4-oxadiazol-5-yl)piperidin-1-yl)methanone (**4g**)*

White solid (130 mg, yield 86%). ^{1}H NMR (300 MHz, $CDCl_3$): δ = 8.08 (m, 1H), 8.00 (m, 1H), 7.49–7.41 (m, 3H), 7.24–7.02 (m, 3H), 5.02, 4.95, 4.77 and 4.37 (4× m, 1H), 3.75–3.10 (m, 3H) 2.41–2.27 (m, 4H), 2.03–1.64 (m, 3H); LC/MS (ESI): *m/z* 382.0 $[M + 1]^+$; Anal. Calcd. for $C_{21}H_{20}ClN_3O_2$: C, 66.05; H, 5.28; N, 11.00. Found: C, 66.12; H, 5.19; N, 10.86.

*4.3.12. (S)-(3-Bromo-2-methylphenyl)(3-(3-phenyl-1,2,4-oxadiazol-5-yl)piperidin-1-yl)methanone (**4h**)*

White solid (156 mg, yield 82%). ^{1}H NMR (400 MHz, $CDCl_3$): δ = 8.09 (m, 1H), 8.01 (m, 1H), 7.60–7.46 (m, 4H), 7.18–7.03 (m, 2H), 4.88, 4.65 and 4.33 (3× m, 1H), 3.75 and 3.47 (2× m, 2H), 3.33 and 3.12 (2× m, 2H), 2.43–2.29 (m, 4H), 2.08–1.73 (m, 3H); LC/MS (ESI): *m/z* 425.8 $[M + H]^+$; HRMS-ESI: *m/z* $[M + Na]^+$ calcd for $C_{21}H_{20}BrN_3NaO_2^+$: 448.0631, found: 448.0621.

*4.3.13. (S)-(3-Iodo-2-methylphenyl)(3-(3-phenyl-1,2,4-oxadiazol-5-yl)piperidin-1-yl)methanone (**4i**)*

White solid (205 mg, yield 87%). ^{1}H NMR (300 MHz, $CDCl_3$): δ = 8.09 (d, *J* = 7.9 Hz, 1H), 8.00 (m, 1H), 7.85 (dd, *J* = 7.8, 7.9 Hz, 1H), 7.51–7.46 (m, 3H), 7.20–7.15 (dd, *J* = 7.8, 8.4 Hz, 1H), 6.89–6.96 (m, 1H), 4.88, 4.63 and 4.32 (3× m, 1H), 3.75–3.07 (m, 4H), 2.45–2.33 (m, 4H), 2.04–1.71 (m, 3H); EI-MS *m/z*: 474 $[M + H]^+$; Anal. Calcd. for $C_{21}H_{20}IN_3O_2$: C, 53.29; H, 4.26; N, 8.88; Found: C, 53.44; H, 4.31; N, 8.63.

*4.3.14. (S)-(3-(3-Phenyl-1,2,4-oxadiazol-5-yl)piperidin-1-yl)(pyridin-2-yl)methanone (**4j**)*

White solid (140 mg, yield 84%). ^{1}H NMR (300 MHz, $CDCl_3$): δ = 8.71 (m, 2H), 8.09–8.00 (m, 2H), 7.50–7.45 (m, 3H), 7.33 (m,

2H), 4.78 and 4.20 (2× m, 1H), 3.89–3.16 (m, 4H), 2.72 (m, 1H), 2.34 (m, 1H), 2.06–1.71 (m, 2H); ^{13}C NMR (100 MHz, $CDCl_3$): δ = 179.20 and 178.74 (1C), 168.33, 168.09, 150.41 (2C), 150.31, 143.30, 131.33, 128.90 (2C), 127.45 (2C), 126.65, 121.11, 49.64 and 47.72 (1C), 44.45 and 42.34 (1C), 35.15 and 34.46 (1C), 28.46 and 28.38 (1C), 24.71 and 23.33 (1C); LC/MS (ESI): *m/z* 334.9 $[M + H]^+$; HRMS-ESI: *m/z* $[M + H]^+$ calcd for $C_{19}H_{19}N_4O_2^+$: 335.1503, found: 335.1502.

4.3.15. (S)-Furan-2-yl(3-(3-phenyl-1,2,4-oxadiazol-5-yl)piperidin-1-yl)methanone (**4k**)

Primrose yellow oil (111 mg, yield 69%). ^{1}H NMR (400 MHz, $CDCl_3$): δ = 8.07–8.05 (m, 2H), 7.50–7.47 (m, 4H), 7.05 (d, *J* = 3.4 Hz, 1H), 6.49 (dd, *J* = 1.8, 3.4 Hz, 1H), 4.77 (m, 1H), 4.44 (m, 1H), 3.51 (br s, 1H), 3.34–3.18 (m, 2H), 2.38 (m, 1H), 2.03–1.90 (m, 2H), 1.75 (m, 1H); ^{13}C NMR (100 MHz, $CDCl_3$): δ = 179.42, 168.31, 159.42, 147.86, 143.79, 131.19, 128.82 (2C), 127.48 (2C), 126.74, 116.63, 111.34, 47.31 (br s, 1C), 45.22 (br s, 1C), 35.27, 28.89, 24.55; LC/MS (ESI): *m/z* 323.9 $[M + H]^+$; HRMS-ESI: *m/z* $[M + H]^+$ calcd for $C_{18}H_{18}N_3O_3^+$: 324.1343, found: 324.1345.

4.3.16. (S)-(1-Methyl-1H-pyrrol-2-yl)(3-(3-phenyl-1,2,4-oxadiazol-5-yl)piperidin-1-yl)methanone (**4l**)

White solid (105 mg, yield 63%). ^{1}H NMR (300 MHz, $CDCl_3$): δ = 8.07–8.04 (m, 2H), 7.49–7.45 (m, 3H), 6.71 (m, 1H), 6.38 (m, *J* = 2.2 Hz, 1H), 6.10–6.08 (dd, *J* = 2.1, 3.5 Hz, 1H), 4.73 (d, *J* = 12.3 Hz, 1H), 4.36 (d, *J* = 12.3 Hz, 1H), 3.77 (s, 3H), 3.53 (m, 1H), 3.40–3.21 (m, 2H), 2.36 (m, 1H), 2.07–1.89 (m, 2H), 1.73 (m, 1H); LC/MS (ESI): *m/z* 336.9 $[M + H]^+$; HRMS-ESI: *m/z* $[M + H]^+$ calcd for $C_{19}H_{21}N_4O_2^+$: 337.1659, found: 337.1664.

4.3.17. (S)-(4,5-Dibromo-1-methyl-1H-pyrrol-2-yl)-[3-(3-phenyl-[1,2,4]oxadiazol-5-yl)-piperidin-1-yl]-methanone (**4m**)

Primrose yellow solid (126 mg, yield 51%). ^{1}H NMR (300 MHz, $CDCl_3$): δ = 8.06–8.03 (m, 2H), 7.54–7.44 (m, 3H), 6.44 (s, 1H), 4.51 (m, 1H), 4.10 (m, 1H), 3.70 (s, 3H), 3.67 (m, 1H), 3.38 (m, 1H), 3.24 (m, 1H), 2.32 (m, 1H), 2.06 (m, 1H), 1.91 (m, 1H), 1.71 (m, 1H); Anal. Calcd. for $C_{19}H_{18}Br_2N_4O_2$: C, 46.18; H, 3.67; N, 11.34; Found: C, 46.06; H, 3.81; N, 11.42.

4.3.18. (S)-(1-Methyl-1H-indol-4-yl)-[3-(3-phenyl-[1,2,4]oxadiazol-5-yl)-piperidin-1-yl]-methanone (**4n**)

White solid (146 mg, yield 76%). ^{1}H NMR (300 MHz, $CDCl_3$): δ = 8.06–8.02 (m, 2H), 7.53–7.41 (m, 3H), 7.37 (d, *J* = 8.3 Hz, 1H), 7.24 (dd, *J* = 7.1, 8.3 Hz, 1H), 7.15 (d, *J* = 7.1 Hz, 1H), 7.09 (d, *J* = 2.6 Hz, 1H),6.47 (d, *J* = 2.6 Hz, 1H), 5.00 and 4.66 (2× m, 1H), 4.22–4.01 (m, 1H), 3.80 (s, 3H), 3.46–3.10 (m, 3H), 2.32 (m, 1H), 2.03–1.89 (m, 2H), 1.74 (m, 1H); LC-MS (ESI): *m/z* 386.9 $[M + 1]^+$; Anal. Calcd. for $C_{23}H_{22}N_4O_2$: C, 71.48; H, 5.74; N, 14.50; Found: C, 71.75; H, 5.87; N, 14.24.

4.3.19. (S)-(1-Methyl-1H-indol-3-yl)(3-(3-phenyl-1,2,4-oxadiazol-5-yl)piperidin-1-yl)methanone (**4o**)

White solid (125 mg, yield 81%). ^{1}H NMR (300 MHz, $CDCl_3$): δ = 8.06–8.03 (m, 2H), 7.71 (d, *J* = 4.5 Hz, 1H), 7.48–7.41 (m, 4H), 7.34–7.19 (m, 3H), 4.68 (d, *J* = 12.0 Hz, 1H), 4.27 (d, *J* = 13.3 Hz, 1H), 3.78 (s, 3H), 3.50 (dd, J_1 = 10.3 Hz, J_2 = 12.7 Hz, 1H), 3.33–3.20 (m, 2H), 2.33 (m, 1H), 2.05–1.83 (m, 2H), 1.70 (m, 1H); LC-MS (ESI): *m/z* 387.0 $[M + 1]^+$; Anal. Calcd. for $C_{23}H_{22}N_4O_2$: C, 71.48; H, 5.74; N, 14.50; Found: C, 71.61; H, 5.66; N, 14.39.

4.3.20. (S)-Cycloheptyl(3-(3-phenyl-1,2,4-oxadiazol-5-yl)piperidin-1-yl)methanone (**4p**)

White solid (138 mg, yield 78%). ^{1}H NMR (300 MHz, $CDCl_3$): δ = 8.08–8.05 (m, 2H), 7.49 (br s, 3H), 4.84 and 4.21 (2× m, 1H), 4.09 and 3.88 (2× m, 1H), 3.69–3.04 (m, 3H), 2.72 (m, 1H), 2.30 (m, 1H), 2.05–1.46 (m, 15H); LC-MS (ESI): 354.0 $[M + 1]^+$; Anal. Calcd. for $C_{21}H_{27}N_3O_2$: C, 71.36; H, 7.70; N, 11.89; Found: C, 71.10; H, 7.93; N, 11.73.

4.3.21. (S)-Cyclohexyl(3-(3-phenyl-1,2,4-oxadiazol-5-yl)piperidin-1-yl)methanone (**4q**)

White solid (108 mg, yield 64%). ^{1}H NMR (400 MHz, $CDCl_3$): δ = 8.08–8.04 (m, 2H), 7.49 (m, 3H), 4.86 and 4.23 (2× m, 1H), 4.11 and 3.91 (2× m, 1H), 3.69–3.05 (m, 3H), 2.57 (m, 1H), 2.30 (m, 1H), 2.03–1.49 (m, 13H); ^{13}C NMR (100 MHz, $CDCl_3$): δ = 179.72 and 179.42 (1C), 174.86 and 174.79 (1C), 168.35 and 168.22 (1C), 131.34 and 131.16 (1C), 128.85 (2C), 127.46 (2C), 126.80 and 126.59 (1C), 47.98 and 45.68 (1C), 44.32 and 41.96 (1C), 40.60 and 40.35 (1C), 35.68 and 34.79 (1C), 29.65 and 29.51 (1C), 29.42 and 29.29 (1C), 28.86 and 28.65 (1C), 25.88 and 25.84 (3C), 25.32 and 23.77 (1C); LC/MS (ESI): *m/z* 340.0 $[M + H]^+$; HRMS-ESI: *m/z* $[M + H]^+$ calcd for $C_{20}H_{26}N_3O_2^+$: 340.2020, found: 340.2022.

4.3.22. (S)-Cyclobutyl(3-(3-phenyl-1,2,4-oxadiazol-5-yl)piperidin-1-yl)methanone (**4r**)

White solid (88 mg, yield 56%). ^{1}H NMR (400 MHz, $CDCl_3$): δ = 8.09–8.06 (m, 2H), 7.52–7.47 (m, 3H), 4.84 and 4.33 (2× m, 1H), 3.98 and 3.71 (2× m, 1H), 3.49–2.94 (m, 4H), 2.43–2.13 (m, 5H), 2.01–1.82 (m, 4H), 1.57 (m, 1H); ^{13}C NMR (100 MHz, $CDCl_3$): δ = 179.71 and 179.36 (1C), 173.27, 168.36 and 168.25 (1C), 131.35 and 131.18 (1C), 128.90 and 128.86 (2C), 127.46 (2C), 126.80 and 126.60 (1C), 47.75 and 45.27 (1C), 44.42 and 42.01 (1C), 37.38 and 37.25 (1C), 35.60 and 34.73 (1C), 28.84 and 28.60 (1C), 25.56 and 25.32 (1C), 25.04, 24.84 and 23.82 (1C), 17.97; EI-MS *m/z*: 312 $[M + H]^+$; LC/MS (ESI): *m/z* 312.0 $[M + H]^+$; HRMS-ESI: *m/z* $[M + Na]^+$ calcd for $C_{18}H_{21}N_3NaO_2^+$: 334.1526, found: 334.1534.

4.3.23. (S)-Cyclopropyl(3-(3-phenyl-1,2,4-oxadiazol-5-yl)piperidin-1-yl)methanone (**4s**)

White solid (78 mg, yield 53%). ^{1}H NMR (400 MHz, $CDCl_3$): δ = 8.09–8.06 (m, 2H), 7.50–7.48 (m, 3H), 4.87 and 4.36 (2× m, 1H), 4.21 (m, 1H), 4.12 and 3.80 (2× m, 1H), 3.28–3.09 (m, 2H), 2.33 (m, 1H), 2.07–1.78 (m, 4H), 1.00–0.98 (m, 2H), 0.80–0.78 (m, 2H); ^{13}C NMR (100 MHz, $CDCl_3$): δ = 179.66 and 179.49 (1C), 172.20, 168.28, 131.26, 128.87, 127.46, 127.35 and 126.64 (1C), 48.23 and 45.90 (1C), 44.96 and 42.58 (1C), 35.45 and 34.67 (1C), 28.89 and 28.52 (1C), 25.15 and 23.61 (1C), 11.11, 7.56 (2C); LC/MS (ESI): *m/z* 298.0 $[M + H]^+$; HRMS-ESI: *m/z* $[M + Na]^+$ calcd for $C_{17}H_{19}N_3NaO_2^+$: 320.1369, found: 320.1370.

4.3.24. (S)-(3-(3-Phenyl-1,2,4-oxadiazol-5-yl)piperidin-1-yl)(2,2,3,3-tetramethylcyclopropyl)methanone (**4t**)

White solid (92 mg, yield 52%). ^{1}H NMR (300 MHz, $CDCl_3$): δ = 8.08–8.06 (m, 2H), 7.49 (br s, 3H), 4.80 and 3.96 (2× m, 1H), 4.27 (m, 1H), 3.53 and 2.92 (2× m, 1H), 3.23–3.05 (m, 2H), 2.31 (m, 1H), 2.03–1.78 (m, 3H), 1.60 (m, 1H), 1.17 (s, 12H); LC/MS (ESI): *m/z* 354.0 $[M + H]^+$; Anal. Calcd. for $C_{21}H_{27}N_3O_2$: C, 71.36; H, 7.70; N, 11.89; Found: C, 71.56; H, 7.91; N, 11.68.

4.3.25. Bicyclo[2.2.1]heptan-2-yl((S)-3-(3-phenyl-1,2,4-oxadiazol-5-yl)piperidin-1-yl)methanone (**4u**)

White solid (120 mg, yield 68%). ^{1}H NMR (300 MHz, $CDCl_3$): δ = 8.08–8.02 (m, 2H), 7.51–7.43 (m, 3H), 5.02–4.31 (m, 1H), 4.24–3.88 (m, 1H), 3.61–3.20 (m, 1H), 3.18–2.88 (m, 3H), 2.38–2.25 (m, 3H), 2.03–1.74 (m, 3H), 1.57–1.27 (m, 8H); Anal. Calcd. for $C_{21}H_{25}N_3O_2$: C, 71.77; H, 7.17; N, 11.96; Found: C, 71.63; H, 7.22; N, 11.76.

4.3.26. (S)-(1-Methylcyclohexyl)(3-(3-phenyl-1,2,4-oxadiazol-5-yl)piperidin-1-yl)methanone (**4v**)

White solid (94 mg, yield 53%). ^{1}H NMR (300 MHz, $CDCl_3$): δ = 8.09–8.06 (m, 1H), 7.49–7.46 (m, 3H), 4.70 (d, *J* = 12.6 Hz, 1H),

4.37 (d, J = 12.6 Hz, 1H), 3.28–3.11 (m, 2H), 2.99 (dd, J_1 = 11.1 Hz, J_2 = 13.3 Hz, 1H), 2.18 (m, 1H), 2.07–1.85 (m, 4H), 1.68–1.31 (m, 9H); Anal. Calcd. for $C_{21}H_{27}N_3O_2$: C, 71.36; H, 7.70; N, 11.89; Found: C, 71.50; H, 7.84; N, 11.98.

4.3.27. (S)-(Adamant-1-yl)(3-(3-phenyl-1,2,4-oxadiazol-5-yl) piperidin-1-yl)methanone (**4w**)

White solid (160 mg, yield 73%). ^{1}H NMR (300 MHz, $CDCl_3$): δ = 8.09–8.06 (m, 2H), 7.53–7.48 (m, 3H), 4.82 (d, J = 9.6 Hz, 1H), 4.50 (d, J = 13.5 Hz, 1H), 3.18–3.14 (m, 2H), 2.98 (m, 1H), 2.34 (m, 1H), 2.05–1.88 (m, 10H), 1.77–1.59 (m, 8H); ^{13}C NMR (100 MHz, $CDCl_3$): δ = 179.66, 176.02, 168.27, 131.20, 128.86 (2C), 127.48 (2C), 126.77, 47.98, 45.98, 39.14 (3C), 36.64 (3C), 35.42, 29.72, 28.89, 28.51 (3C), 24.94; LC/MS (ESI): m/z 392.0 $[M + H]^+$; HRMS-ESI: m/z $[M + H]^+$ calcd for $C_{24}H_{30}N_3O_2^+$: 392.2333, found: 392.2339.

4.4. Docking study

The crystal structure 3G49 was downloaded from Protein Data Bank (PDB) database [21]. Then, Autodock toolkit was used to prepare the models for docking study [20]. For that, the crystal water was deleted, hydrogen atoms were added, and Gasteiger charge model was used for protein and NAD. Totally, two monomers and one NAD molecule were included in receptor model for docking. The ligand **3** and **4a** were built and added the Gasteiger charges. Then the receptor and ligands were saved in PDBQT format for Vina program. The default parameters of Vina were used for docking simulation, except for the parameter *exhaustiveness* was set to 11 to enable the Vina to explore more search space. And finally, the lowest energy binding conformations were analyzed and illustrated with Pymol program.

4.5. Biological assays

Enzymatic activities of compounds against h11β-HSD1 and m11β-HSD1 and h11β-HSD2 were determined by the scintillation proximity assay (SPA) using microsomes containing 11β-HSDs according to previous studies [18]. Briefly, the full-length cDNAs of human or mouse 11β-HSDs were isolated from cDNA libraries provided by NIH Mammalian Gene Collection and cloned into pcDNA3 expression vectors (Invitrogen, Carlsbad, CA, USA) by PCR. HEK-293 cells were transfected with the pcDNA3-derived expression plasmids and selected by cultivation at the presence of 700 μg/mL G418. The microsomal fraction over-expressing 11β-HSDs was prepared from the HEK-293 cells stably transfected with 11β-HSDs and used as the enzyme source for SPA. The assay was performed in a 96-well microtiter plate. Compounds with different concentrations were added, followed by adding 80 μL of 50 mM HEPES buffer, pH 7.4 containing 25 nM cortisone [1,2-^{3}H(N)] (Amersham, Buckinghamshire, UK) and 1.25 mM NADPH (for 11β-HSD1 assay) or 12.5 nM cortisol [1,2,6,7-^{3}H(N)] (Amersham, Buckinghamshire, UK) and 0.625 mM NAD (for 11β-HSD2 assay).

4.6. In vitro DMPK evaluation

Reactions were initiated by the addition of enzyme preparations as microsome fractions from HEK293 cells in a final concentration of 80 μg/mL for 11β-HSD1. Following 60 min incubation at 37 °C, the reaction was stopped by adding 35 μL of 10 mg/mL protein A-coated SPA beads (GE, Piscataway, NJ, USA) suspended in Superblock® Blocking Buffer (Pierce, Rockford, IL) with 3 μg/mL of murine monoclonal cortisol antibody (East Coast Biologics, North Berwick, Maine, USA)and 314 μM glycyrrhetinic acid (Sigma–Aldrich, St. Louis, MO). The plates were incubated under plastic film on an orbital shaker for 120 min at room temperature before counting. The amount of [^{3}H] cortisol generated by 11β-HSD1 was captured on the beads and measured in a microplate liquid scintillation counter. Percent inhibition was calculated relative to noninhibited control. Data were obtained from at least three independent experiments. IC_{50} values were calculated by using Prism Version 4 (GraphPad Software, San Diego, CA).

Microsomes (Human microsome: Xenotech, Lot No.H0610; Rat microsome: Xenotech, Lot No. R1000) (0.5 mg/mL) were preincubated with 1 μM test compound for 5 min at 37 °C in 0.1 M phosphate buffer (pH 7.4) with 1 mM EDTA, and 5 mM $MgCl_2$. The reactions were initiated by adding prewarmed cofactors (1 mM NADPH). After 0, 5, 10, and 30 min incubations at 37 °C, the reactions were stopped by adding an equal volume of cold acetonitrile. The samples were vortexed for 10 min and then centrifuged at 10,000 *g* for 10 min. Supernatants were analyzed by LC/MS/MS for the amount of parent compound remaining, and the corresponding loss of parent compound also determined by LC/MS/MS.

The CYP enzymatic activities were characterized based on their probe reactions: CYP3A4 (midazolam 1-hydroxylation), CYP2D6 (dextromethorphan *O*-demethylation), and CYP1A2 (phenacetin *O*-deethylation). Incubation mixtures were prepared in a total volume of 100 μl as follows: 0.2 mg/mL microsome (Human microsome: Xenotech, Lot No.H0610), NADPH (1 mM), 100 mM phosphate buffer (pH 7.4), probe substrates cocktail (midazolam 5 μM, dextromethorphan 5 μM, phenacetin 100 μM) and 10 μM tested compound or positive control cocktail (ketoconazole 10 μM, quinidine 10 μM, α-naphthoflavone 10 μM or negative control (PBS)). The final concentration of organic reagent in incubation mixtures was less than 1% v/v. There was a 5 min preincubation period at 37 °C before the reaction was initiated by adding a NADPH-generating system. Reactions were conducted for 20 min for CYP3A4, CYP2D6 and CYP1A2. For each probe drug, the percentage of metabolite conversion was less than 20% of substrate added. The inhibition rate was calculated as: (The formation of the metabolite of probe substrates with 10 μM tested compound)/(The formation of the metabolite of probe substrates with PBS) × 100%.

The samples for the time-dependent inactivation screening assay were preincubated for 0, 5, 10, 20 min at 37 °C with 0.2 mg/mL human microsome (Xenotech, Lot No.H0610) and 10 μM test compound or positive control (troleandomycin 10 μM, paroxetine 10 μM and furafylline 10 μM) with or without 1 mM NADPH. The percentage of remaining activity of CYP3A4, CYP2D6, and CYP1A2 was measured by the formation of the metabolite of their marker substrates: midazolam, dextromethorphan and phenacetin at single concentration approximating their Km values (midazolam 5 μM, dextromethorphan 5 μM, phenacetin 100 μM). The percentage of remaining activity of microsomes preincubated with NADPH was compared with that of microsomes without preincubation.

Acknowledgments

We thank Dr. David Burk for critical reading the manuscript and Prof. Ying Leng of SIMM for the 11β-HSD1 assay. We are grateful for financial support from New Drug Creation Project of the National Science and Technology Major Foundation of China (project 2010ZX09401-404), to Shanghai Pharmaceutical Holding, Shanghai Postdoctoral Sustentation Fund, China (grant No. 07R214213 to GX. Xia) and Program of Excellent Young Scientist of Chinese Academy of Sciences (Grant to BX: KSCX2-EW-Q-3-01).

Appendix A. Supplementary data

Supplementary data related to this article can be found at http://dx.doi.org/10.1016/j.ejmech.2012.12.059.

References

[1] M. Wang, Handb. Inhibitors of 11β-hydroxysteroid dehydrogenase type 1 in antidiabetic therapy, Exp. Pharmacol. 203 (2011) 127–146.

[2] R. Kahn, J. Buse, E. Ferrannini, M. Stern, The metabolic syndrome: time for a critical appraisal. Joint statement from the American Diabetes Association and the European Association for the Study of Diabetes, Diabetologia 48 (2005) 1684–1699.

[3] A.J. Rose, A. Vegiopoulos, S. Herzig, Role of glucocorticoids and the glucocorticoid receptor in metabolism: insights from genetic manipulations, J. Steroid. Biochem. Mol. Biol. 122 (2010) 10–20.

[4] J.W. Tomlinson, P.M. Stewart, Modulation of glucocorticoid action and the treatment of type-2 diabetes, Best Pract. Res. Clin. Endocrinol. Metab. 21 (2007) 607–619.

[5] R. Rosmond, The glucocorticoid receptor gene and its association to metabolic syndrome, Obes. Res. 10 (2002) 1078–1086.

[6] E. Saiah, The role of 11beta-hydroxysteroid dehydrogenase in metabolic disease and therapeutic potential of 11beta-hsd1 inhibitors, Curr. Med. Chem. 15 (2008) 642–649.

[7] M. Wamil, J.R. Seckl, Inhibition of 11beta-hydroxysteroid dehydrogenase type 1 as a promising therapeutic target, Drug Discov. Today 12 (2007) 504–520.

[8] C. Hale, M. Wang, Development of 11beta-HSD1 inhibitors for the treatment of type 2 diabetes, Mini. Rev. Med. Chem. 8 (2008) 702–710.

[9] A. Tiwari, INCB-13739, an 11beta-hydroxysteroid dehydrogenase type 1 inhibitor for the treatment of type 2 diabetes, IDrugs 13 (2010) 266–275.

[10] T. Barf, J. Vallgaårda, R. Emond, C. Haeggstroem, G. Kurz, A. Nygren, V. Larwood, E. Mosialou, K. Axelsson, R. Olsson, L. Engblom, N. Edling, Y. Roenquist-Nii, B. Oehman, P. Alberts, L. Abrahmsen, Arylsulfonamidothiazoles as a new class of potential antidiabetic drugs. Discovery of potent and selective inhibitors of the 11beta-hydroxysteroid dehydrogenase type 1, J. Med. Chem. 45 (2002) 3813–3815.

[11] H. Cheng, J. Hoffman, P. Le, S.K. Nair, S. Cripps, J. Matthews, C. Smith, M. Yang, S. Kupchinsky, K. Dress, M. Edwards, B. Cole, E. Walters, C. Loh, J. Ermolieff, A. Fanjul, G.B. Bhat, J. Herrera, T. Pauly, N. Hosea, G. Paderes, P. Rejto, The development and SAR of pyrrolidine carboxamide 11beta-HSD1 inhibitors, Bioorg. Med. Chem. Lett. 20 (2010) 2897–2902.

[12] A. Hermanowski-Vosatka, J.M. Balkovec, K. Cheng, H.Y. Chen, M. Hernandez, G.C. Koo, C.B. Le Grand, Z. Li, J.M. Metzger, S.S. Mundt, H. Noonan, C.N. Nunes, S.H. Olson, B. Pikounis, N. Ren, N. Robertson, J.M. Schaeffer, K. Shah, M.S. Springer, A.M. Strack, M. Strowski, K. Wu, T. Wu, J. Xiao, B.B. Zhang, S.D. Wright, R. Thieringer, 11beta-HSD1 inhibition ameliorates metabolic syndrome and prevents progression of atherosclerosis in mice, J. Exp. Med. 202 (2005) 517–527.

[13] M.H. Veéniant, C. Hale, R.W. Hungate, K. Gahm, M.G. Emery, J. Jona, S. Joseph, J. Adams, A. Hague, G. Moniz, J. Zhang, M.D. Bartberger, V. Li, R. Syed, S. Jordan, R. Komorowski, M.M. Chen, R. Cupples, K.W. Kim, D.J. Jean, L. Johansson, M.A. Henriksson, M. Williams, J. Vallgaårda, C. Fotsch, M. Wang, Discovery of a potent, orally active 11beta-hydroxysteroid dehydrogenase type 1 inhibitor for clinical study: identification of (*S*)-2-((1*S*,2*S*,4*R*)-bicyclo[2.2.1]heptan-2-ylamino)-5-isopropyl-5-methylthiazol-4(5*H*)-one (AMG 221), J. Med. Chem. 53 (2010) 4481–4487.

[14] J. Rosenstock, S. Banarer, V.A. Fonseca, S.E. Inzucchi, W. Sun, W. Yao, G. Hollis, R. Flores, R. Levy, W.V. Williams, J.R. Seckl, R. Huber, Diabetes Care 33 (2010) 1516–1522.

[15] R. Courtney, P.M. Stewart, M. Toh, M.N. Ndongo, R.A. Calle, B. Hirshberg, Modulation of 11beta-hydroxysteroid dehydrogenase (11betaHSD) activity biomarkers and pharmacokinetics of PF-00915275, a selective 11betaHSD1 inhibitor, J. Clin. Endocrinol. Metab. 93 (2008) 550–556.

[16] P.U. Feig, S. Shah, A. Hermanowski-Vosatka, D. Plotkin, M.S. Springer, S. Donahue, C. Thach, E.J. Klein, E. Lai, K.D. Kaufman, Effects of an 11β-hydroxysteroid dehydrogenase type 1 inhibitor, MK-0916, in patients with type 2 diabetes mellitus and metabolic syndrome, Diabetes Obes. Metab. 13 (2011) 498–504.

[17] J.S. Scott, S.S. Bowker, J. Deschoolmeester, S. Gerhardt, D. Hargreaves, E. Kilgour, A. Lloyd, R.M. Mayers, W. McCoull, N.J. Newcombe, D. Ogg, M.J. Packer, A. Rees, J. Revill, P. Schofield, N. Selmi, J.G. Swales, P.R. Whittamore, Discovery of a potent, selective, and orally bioavailable acidic 11β-hydroxysteroid dehydrogenase type 1 (11β-HSD1) inhibitor: discovery of 2-[(3*S*)-1-[5-(cyclohexylcarbamoyl)-6-propylsulfanylpyridin-2-yl]-3-piperidyl]acetic acid (AZD4017), J. Med. Chem. 55 (2012) 5951–5964.

[18] G. Xia, L. Liu, M. Xue, H. Liu, J. Yu, P. Li, Q. Chen, B. Xiong, X. Liu, J. Shen, Discovery of novel sulfonamides as potent and selective inhibitors against human and mouse 11β-hydroxysteroid dehydrogenase type 1, Mol. Cell. Endocrinol. 358 (2012) 46–52.

[19] M.D. McBriar, J.W. Clader, I. Chu, R.A. Del Vecchio, L. Favreau, W.J. Greenlee, L.A. Hyde, A.A. Nomeir, E.M. Parker, D.A. Pissarnitski, L. Song, L. Zhang, Z. Zhao, Discovery of amide and heteroaryl isosteres as carbamate replacements in a series of orally active gamma-secretase inhibitors, Bioorg. Med. Chem. Lett. 18 (2008) 215–219.

[20] O. Trott, A.J. Olson, AutoDock Vina: improving the speed and accuracy of docking with a new scoring function, efficient optimization, and multithreading, J. Comput. Chem. 31 (2010) 455–461.

[21] M. Siu, T.O. Johnson, Y. Wang, S.K. Nair, W.D. Taylor, S.J. Cripps, J.J. Matthews, M.P. Edwards, T.A. Pauly, J. Ermolieff, A. Castro, N.A. Hosea, A. LaPaglia, A.N. Fanjul, J.E. Vogel, *N*-(Pyridin-2-yl) arylsulfonamide inhibitors of 11beta-hydroxysteroid dehydrogenase type 1: discovery of PF-915275, Bioorg. Med. Chem. Lett. 19 (2009) 3493–3497.